Composites Research

Vol. 30, No. 6, 343-349 (2017)
DOI: http://dx.doi.org/10.7234/composres.2017.30.6.343
ISSN 2288-2103(Print), ISSN 2288-2111(Online)

Paper

Multifield Variational Finite Element Sectional Analysis of Composite Beams

Manoj Kumar Dhadwal*, Sung Nam Jung*†

ABSTRACT: A multifield variational formulation is developed for the finite element (FE) cross-sectional analysis of composite beams. The cross-sectional warping displacements and sectional stresses are considered to be the primary variables through the application of Reissner's partially mixed principle. The warping displacements are modeled using generic FE shape functions with nonlinear distribution over the beam section. A generalized Timoshenko level stiffness matrix is derived which incorporates the effects of elastic couplings, transverse shear, and Poisson's deformations. The accuracy of the present analysis is validated for the stiffness constants and elastostatic responses of composite box beams which correlate well with the experimental data and other state-of-the-art approaches.

Key Words: Composite beam, Cross-section, Multifield principle, 3D warping

1. INTRODUCTION

Composite structures offer a wide variety of advantages in various engineering fields due to their high stiffness-to-weight ratio. The composite materials provide a convenient way to tailor the structural characteristics by defining the required ply layup. Beam theories have gained a lot of attention in the past decades due to the efficient modeling and analysis of composite slender structures. The three-dimensional (3D) analysis of composite beams is generally decomposed into two-dimensional (2D) sectional and one-dimensional (1D) beam analyses [1,2]. Such a decomposition approach is useful for the preliminary design and optimization of slender composite structures.

Beam cross-sectional analyses are mainly categorized into FE and analytical formulations based on the implementation. The former offers advantage in that any arbitrary geometry with complex material distribution can be modeled in detail while the latter is limited to only simple cross-sections. Giavotto *et al.* [3] developed a FE cross-sectional analysis for generally anisotropic beams based on central and extremity solutions. The central solution was used to compute a Timoshenko level stiffness matrix with elastic couplings. Cesnik and Hodges [4] proposed a variational asymptotic beam sectional analysis to compute stiffness constants formulated based on the variational asymptotic method of Berdischevsky [5]. Chandra *et al.* [6] and Chandra and Chopra [7] developed an analytical formulation with simple expressions for sectional stiffness constants. They also conducted experimental tests to investigate the effect of elastic couplings on the 1D elastostatic response of composite beams and blades. Jung *et al.* [8] presented a mixed shell-wall based analytical force-displacement approach to determine the sectional stiffness constants at Timoshenko-Vlasov level.

Most of the studies mentioned previously adopted a displacement-based approach with displacements as the only primary variables which typically results in low accuracy of stresses. Multifield formulations as proposed by Reissner [9] involving stresses as additional unknown variables can overcome this limitation with more computational effort. In addition, implementation of cross-sectional formulation into a FE analysis can offer the accurate modeling of complex geometric features and composite material layups of beams.

The present work deals with the development of a FE based multifield variational sectional analysis code (MVSAC) for nonhomogeneous anisotropic beams with arbitrary geometry

Received 3 August 2017, received in revised form 26 December 2017, accepted 27 December 2017

*Department of Aerospace Information Engineering, Konkuk University
*†Department of Aerospace Information Engineering, Konkuk University, Corresponding author (E-mail: snjung@konkuk.ac.kr)

and material distribution. The sectional stresses (called as *reactive stresses* [9]) are assumed to be unknowns in addition to 3D sectional warping displacements. The transverse shear and Poisson's deformation effects are inherently taken into account through the 3D warping. A 6×6 generalized Timoshenko stiffness matrix is obtained incorporating the classical and non-classical elastic couplings. The stiffness constants and 1D elastostatic response computed by the present analysis is validated for composite beams with elastic couplings.

2. MULTIFIELD CROSS-SECTIONAL ANALYSIS

The present formulation is applicable for straight and prismatic beams. The schematic of the beam cross-section is shown in Fig. 1, indicating sectional warping and beam generalized displacements. The strain-displacement and semi-inverted material constitutive relations are derived first which are discretized using FE shape functions. The governing equations are formulated to solve for the 3D warping and sectional stresses which are utilized to determine a generalized 6×6 Timoshenko stiffness matrix. A brief description of the present multifield formulation is provided next.

2.1 Kinematical relations

The 3D displacements **u** of an arbitrary point on the beam cross-section are described as the sum of the beam reference line displacements $\mathbf{u}_b = [u_1 \;\; u_2 \;\; u_3]^T$ and the sectional warping displacements $\Psi = [\psi_1 \;\; \psi_2 \;\; \psi_3]^T$, given as

$$\mathbf{u} = \mathbf{u}_b + \Psi \tag{1}$$

where the beam reference line displacements are defined as

$$\mathbf{u}_b = \mathbf{B}\mathbf{q} \tag{2}$$

with **q** and **B** given by

$$\mathbf{q} = \begin{bmatrix} u_1^0 & u_2^0 & u_3^0 & \phi_1 & \phi_2 & \phi_3 \end{bmatrix}^T$$

$$\mathbf{B} = \begin{bmatrix} 1 & 0 & 0 & 0 & \xi_3 & -\xi_2 \\ 0 & 1 & 0 & -\xi_3 & 0 & 0 \\ 0 & 0 & 1 & \xi_2 & 0 & 0 \end{bmatrix} \tag{3}$$

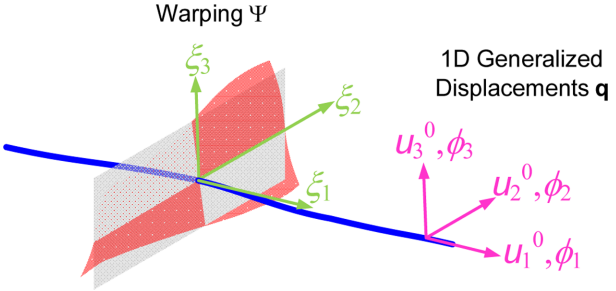

Fig. 1. Flowchart for the present cross-sectional analysis

Here, u_1^0, u_2^0, u_3^0 represent the translations, and ϕ_1 ϕ_2 ϕ_3 represent the rotations of the beam cross-section.

The warping displacements defined in Eq. (1) are six times redundant which can be eliminated through constraints defined in [10], given as

$$\int_A \mathcal{D}_w \Psi \, dA = \mathbf{0} \tag{4}$$

where A denotes the cross-sectional area, and the operator matrix $\mathcal{D}_w$ is given by

$$\mathcal{D}_w = \begin{bmatrix} 1 & 0 & 0 \\ 0 & 1 & 0 \\ 0 & 0 & 1 \\ 0 & -\partial/\partial\xi_3 & \partial/\partial\xi_2 \\ \partial/\partial\xi_3 & 0 & -\partial/\partial\xi_1 \\ -\partial/\partial\xi_2 & \partial/\partial\xi_1 & 0 \end{bmatrix} \tag{5}$$

With the assumptions of small local rotations and small strains at the cross-sectional level, the linear strain-displacement relations are stated as

$$\varepsilon_s^a = \mathbf{B}\Gamma + \mathcal{L}_s^s \Psi + \Psi' \tag{6a}$$

$$\varepsilon_n^a = \mathcal{L}_s^n \Psi \tag{6b}$$

where the subscript s represents the sectional stresses, the subscript n indicates the stresses on the planes normal to the cross-section, the superscript a indicates the active components computed through above strain-displacement relations, and ()' denotes the derivative with respect to the axial coordinate ξ_1. The variable Γ represents the generalized strain measures, and $\mathcal{L}_s^s$ and $\mathcal{L}_s^n$ are the operator matrices defined as

$$\Gamma = \begin{bmatrix} \gamma_1 & \gamma_2 & \gamma_3 & \kappa_1 & \kappa_2 & \kappa_3 \end{bmatrix}^T = \mathcal{L}_q \mathbf{q} + \mathbf{q}' \tag{7}$$

$$\mathcal{L}_s^s = \begin{bmatrix} 0 & 0 & 0 \\ \partial/\partial\xi_2 & 0 & 0 \\ \partial/\partial\xi_3 & 0 & 0 \end{bmatrix}, \quad \mathcal{L}_s^n = \begin{bmatrix} 0 & \partial/\partial\xi_2 & 0 \\ 0 & 0 & \partial/\partial\xi_3 \\ 0 & \partial/\partial\xi_3 & \partial/\partial\xi_2 \end{bmatrix}$$

Here, γ_1 is the extensional strain, γ_2 and γ_3 are the transverse shear strains, κ_1 is the twist curvature, κ_3 and κ_3 are the bending curvatures. The matrix $\mathcal{L}_q$ is given as

$$\mathcal{L}_q = \begin{bmatrix} 0 & 0 & 0 & 0 & 0 & 0 \\ 0 & 0 & 0 & 0 & 0 & -1 \\ 0 & 0 & 0 & 0 & 1 & 0 \\ 0 & 0 & 0 & 0 & 0 & 0 \\ 0 & 0 & 0 & 0 & 0 & 0 \\ 0 & 0 & 0 & 0 & 0 & 0 \end{bmatrix} \tag{8}$$

2.2 Semi-inverted material constitutive relations

For a linearly elastic anisotropic material, the constitutive relations in the material coordinate system are defined using generalized Hooke's law as

$$\sigma_m = \mathbf{C}_m \varepsilon_m \tag{9}$$

where σ_m denotes the stress vector, ε_m denotes the strain vector, and $\mathbf{C}_m$ is the material constitutive matrix. These constitutive relations can be transformed to the beam coordinate system through transformation by fiber angle and fiber plane angle for composite materials. The sectional stresses (one normal and two transverse shear components) in the present formulation are considered to be unknowns, and hereafter called as *reactive sectional stresses*. Therefore, the material constitutive relations are expressed in a semi-inverted form as given by

$$\begin{Bmatrix} \varepsilon_s^r \\ \sigma_n^a \end{Bmatrix} = \begin{bmatrix} \overline{\mathbf{C}}_{ss} & \overline{\mathbf{C}}_{sn} \\ -\overline{\mathbf{C}}_{sn}^T & \overline{\mathbf{C}}_{nn} \end{bmatrix} \begin{Bmatrix} \sigma_s^r \\ \varepsilon_n^a \end{Bmatrix} \tag{10}$$

where the superscript *r* denotes the reactive sectional stresses which are directly computed from the multifield formulation whereas the superscript *a* denotes the remaining active stresses computed through kinematical relations.

2.3 Finite element discretization

The warping displacements and the reactive sectional stresses are discretized using isoparametric FE shape functions as

$$\Psi(\xi_1, \xi_2, \xi_3) = \mathbf{N}_\psi(\xi_2, \xi_3)\, \Lambda(\xi_1) \tag{11a}$$

$$\sigma_s^r(\xi_1, \xi_2, \xi_3) = \mathbf{N}_\sigma(\xi_2, \xi_3)\, \Upsilon(\xi_1) \tag{11b}$$

where Λ and Υ are respectively the nodal values of warping displacements and reactive stresses, and $\mathbf{N}_\psi$ and $\mathbf{N}_\sigma$ are the respective FE shape functions.

The warping constraints from Eq. (4) are expressed in discretized form as

$$\left(\int_A \mathcal{D}_w \mathbf{N}_\psi \, dA\right)\Lambda = \mathbf{D}_\psi \Lambda = \mathbf{0} \tag{12}$$

where $\mathbf{D}_\psi$ is the warping constraint matrix.

2.4 Governing equations

The present multifield formulation considers sectional stresses and displacements as primary variables. The variation of total energy per unit beam length is expressed as

$$\delta\Pi_R = \delta U_s - \delta W_s = \delta L \tag{13}$$

where δU_s is the variation of cross-sectional strain energy, δW is the variation of external work due to applied loads, and δL is the variation of warping constraints obtained from Eq. (12) using Lagrange multipliers $\mathbf{\Theta}_\psi$, as given by

$$\delta L = -\delta\Lambda^T \mathbf{D}_\psi^T \Theta_\psi - \delta\Theta_\psi^T (\mathbf{D}_\psi \Lambda) \tag{14}$$

The generalized form of Reissner's semi-complimentary energy functional Φ_R [9] is stated as

$$\Phi_R = \frac{1}{2}\left((\varepsilon_n^a)^T \sigma_n^a - (\sigma_s^r)^T \varepsilon_s^r\right) \tag{15}$$

The cross-sectional strain energy is defined using Φ_R as

$$U_s = \int_A \left[\Phi_R + (\varepsilon_s^r)^T \sigma_s^r\right] dA \tag{16}$$

The active strains ε_s^a from kinematical relations and the reactive strains ε_s^r from semi-inverted material constitutive relations must be compatible, implying $\varepsilon_s^r = \varepsilon_s^a$. The variation of sectional strain energy is then obtained as

$$\delta U_s = \int_A \left[(\delta\varepsilon_n^a)^T \sigma_n^a + (\delta\varepsilon_s^a)^T \sigma_s^r + (\delta\sigma_s^r)^T \left(\varepsilon_s^a - \varepsilon_s^r\right)\right] dA \tag{17}$$

Substituting Eqs. (6), (10), and (11) into the above equation, the sectional strain energy becomes

$$\delta U_s = \begin{Bmatrix} \delta\Lambda' \\ \delta\Upsilon \\ \delta\Lambda \\ \delta\Gamma \\ \delta\Theta_\psi \end{Bmatrix}^T \begin{bmatrix} \mathbf{0} & \mathbf{A} & \mathbf{0} & \mathbf{0} & \mathbf{0} \\ \mathbf{A}^T & -\mathbf{H} & \mathbf{G}^T & \mathbf{R} & \mathbf{0} \\ \mathbf{0} & \mathbf{G} & \mathbf{E} & \mathbf{0} & \mathbf{0} \\ \mathbf{0} & \mathbf{R}^T & \mathbf{0} & \mathbf{0} & \mathbf{0} \\ \mathbf{0} & \mathbf{0} & \mathbf{0} & \mathbf{0} & \mathbf{0} \end{bmatrix} \begin{Bmatrix} \Lambda' \\ \Upsilon \\ \Lambda \\ \Gamma \\ \Theta_\psi \end{Bmatrix} \tag{18}$$

where the matrices **A**, **E**, **G**, **H**, and R include the couplings due to geometry and material distribution of the beam section, given as

$$\mathbf{A} = \int_A \mathbf{N}_\psi^T \mathbf{N}_\sigma \, dA, \quad \mathbf{E} = \int_A \left(\mathcal{L}_s^n \mathbf{N}_\psi\right)^T \overline{\mathbf{C}}_{nn} \mathcal{L}_s^n \mathbf{N}_\psi \, dA$$

$$\mathbf{G} = \int_A \left(\mathcal{L}_s^n \mathbf{N}_\psi - \overline{\mathbf{C}}_{sn} \mathcal{L}_s^n \mathbf{N}_\psi\right)^T \mathbf{N}_\sigma \, dA$$

$$\mathbf{H} = \int_A \mathbf{N}_\sigma^T \overline{\mathbf{C}}_{ss} \mathbf{N}_\sigma \, dA, \quad \mathbf{R} = \int_A \mathbf{N}_\sigma^T \mathbf{B} \, dA \tag{19}$$

The sectional stress resultants are defined as

$$\mathbf{F} = \int_A \mathbf{B}^T \sigma_s \, dA \tag{20}$$

where

$$\mathbf{F} = \begin{bmatrix} F_1 & F_2 & F_3 & M_1 & M_2 & M_3 \end{bmatrix}^T \tag{21}$$

Here, F_1 indicates the extensional force, F_2 and F_3 represent the transverse shear forces, M_1 represents the torsional moment, and M_2 and M_3 denote the bending moments.

Neglecting surface and body forces, the external work per

unit beam length is stated as

$$W_s = \int_A \left(\mathbf{u}^T \sigma_s\right)' dA \tag{22}$$

Substituting Eqs. (1), (2), (11), and (20) into the above equation, the variation of external work can be obtained as

$$\delta W_s = \begin{Bmatrix} \delta\Lambda' \\ \delta\Upsilon \\ \delta\Lambda \\ \delta\Gamma \\ \delta\Theta_\psi \end{Bmatrix}^T \begin{Bmatrix} \mathbf{P} \\ \mathbf{0} \\ \mathbf{P}' \\ \mathbf{F} \\ \mathbf{0} \end{Bmatrix} + \delta\mathbf{q}^T \left(\mathbf{F}' - \mathcal{L}_q^T \mathbf{F}\right) \tag{23}$$

where

$$\mathbf{P} = \int_A \mathbf{N}_\psi^T \sigma_s \, dA, \quad \mathbf{P}' = \int_A \mathbf{N}_\psi^T (\sigma_s)' dA \tag{24}$$

2.5 Warping solution and stiffness matrix

The warping displacements and the reactive stresses are approximated as linear functions of sectional stress resultants, as given by

$$\Lambda = \tilde{\Lambda}\mathbf{F}, \quad \Upsilon = \tilde{\Upsilon}\mathbf{F}, \quad \Gamma = \tilde{\Gamma}\mathbf{F}, \quad \Theta_\psi = \tilde{\Theta}_\psi \mathbf{F} \tag{25}$$

$$\Lambda' = \tilde{\Lambda}_p\mathbf{F}, \quad \Upsilon' = \tilde{\Upsilon}_p\mathbf{F}, \quad \Gamma' = \tilde{\Gamma}_p\mathbf{F}, \quad \Theta'_\psi = \tilde{\Theta}_{\psi p}\mathbf{F} \tag{26}$$

where $\tilde{\Lambda}$ and $\tilde{\Upsilon}$ respectively indicate the nodal values of warping and reactive stress coefficients, and $\tilde{\Gamma}$ indicates the beam strain measure coefficients which are constant over the sectional area. The variables with subscript p represent the nodal coefficients corresponding to the derivatives of generalized strain measures. The coefficients matrices incorporate the contributions from extension, shear, bending and torsion of the beam section.

Using the approximations of warping and reactive stresses from Eq. (11), and substituting Eqs. (14), (18), and (23) into Eq. (13), the equilibrium equations are obtained as

$$\begin{bmatrix} -\mathbf{H} & \mathbf{G}^T & \mathbf{R} & \mathbf{0} \\ \mathbf{G} & \mathbf{E} & \mathbf{0} & \mathbf{D}_\psi^T \\ \mathbf{R}^T & \mathbf{0} & \mathbf{0} & \mathbf{0} \\ \mathbf{0} & \mathbf{D}_\psi & \mathbf{0} & \mathbf{0} \end{bmatrix} \begin{bmatrix} \tilde{\Upsilon}_p \\ \tilde{\Lambda}_p \\ \tilde{\Gamma}_p \\ \tilde{\Theta}_{\psi p} \end{bmatrix} = \begin{bmatrix} \mathbf{0} \\ \mathbf{0} \\ \mathcal{L}_q^T \\ \mathbf{0} \end{bmatrix} \tag{27a}$$

$$\begin{bmatrix} -\mathbf{H} & \mathbf{G}^T & \mathbf{R} & \mathbf{0} \\ \mathbf{G} & \mathbf{E} & \mathbf{0} & \mathbf{D}_\psi^T \\ \mathbf{R}^T & \mathbf{0} & \mathbf{0} & \mathbf{0} \\ \mathbf{0} & \mathbf{D}_\psi & \mathbf{0} & \mathbf{0} \end{bmatrix} \begin{bmatrix} \tilde{\Upsilon} \\ \tilde{\Lambda} \\ \tilde{\Gamma} \\ \tilde{\Theta}_\psi \end{bmatrix} = \begin{bmatrix} \mathbf{0} & -\mathbf{A}^T & \mathbf{0} & \mathbf{0} \\ \mathbf{A} & \mathbf{0} & \mathbf{0} & \mathbf{0} \\ \mathbf{0} & \mathbf{0} & \mathbf{0} & \mathbf{0} \\ \mathbf{0} & \mathbf{0} & \mathbf{0} & \mathbf{0} \end{bmatrix} \begin{bmatrix} \tilde{\Upsilon}_p \\ \tilde{\Lambda}_p \\ \tilde{\Gamma}_p \\ \tilde{\Theta}_{\psi p} \end{bmatrix} + \begin{bmatrix} \mathbf{0} \\ \mathbf{0} \\ \mathbf{I} \\ \mathbf{0} \end{bmatrix} \tag{27b}$$

The warping and reactive stress coefficients are solved using the above set of equations.

The strain energy variation from Eq. (18) can then be updated as

$$\delta U_s = \delta\mathbf{F}^T \begin{bmatrix} \tilde{\Lambda}_p \\ \tilde{\Upsilon} \\ \tilde{\Lambda} \\ \tilde{\Gamma} \end{bmatrix}^T \begin{bmatrix} \mathbf{0} & \mathbf{A} & \mathbf{0} & \mathbf{0} \\ \mathbf{A}^T & -\mathbf{H} & \mathbf{G}^T & \mathbf{R} \\ \mathbf{0} & \mathbf{G} & \mathbf{E} & \mathbf{0} \\ \mathbf{0} & \mathbf{R}^T & \mathbf{0} & \mathbf{0} \end{bmatrix} \begin{bmatrix} \tilde{\Lambda}_p \\ \tilde{\Upsilon} \\ \tilde{\Lambda} \\ \tilde{\Gamma} \end{bmatrix} \mathbf{F} \tag{28}$$

The external work variation can be expressed in terms of generalized Timoshenko like sectional stiffness matrix as

$$\delta W_s = \delta\Gamma^T \mathbf{F} = \delta\mathbf{F}^T \mathbf{K}^{-1} \mathbf{F} \tag{29}$$

Using the energy principle defined in Eq. (13), the 6×6 Timoshenko like stiffness matrix is determined as

$$\mathbf{K} = \left(\begin{bmatrix} \tilde{\Lambda}_p \\ \tilde{\Upsilon} \\ \tilde{\Lambda} \\ \tilde{\Gamma} \end{bmatrix}^T \begin{bmatrix} \mathbf{0} & \mathbf{A} & \mathbf{0} & \mathbf{0} \\ \mathbf{A}^T & -\mathbf{H} & \mathbf{G}^T & \mathbf{R} \\ \mathbf{0} & \mathbf{G} & \mathbf{E} & \mathbf{0} \\ \mathbf{0} & \mathbf{R}^T & \mathbf{0} & \mathbf{0} \end{bmatrix} \begin{bmatrix} \tilde{\Lambda}_p \\ \tilde{\Upsilon} \\ \tilde{\Lambda} \\ \tilde{\Gamma} \end{bmatrix} \right)^{-1} \tag{30}$$

The above stiffness matrix considers the elastic couplings effects including transverse shear and Poisson's deformations, and can be fully populated for generally anisotropic beams.

2.6 Finite element implementation

The present multifield formulation is implemented into a FE code called MVSAC with flowchart as shown in Fig. 2. The discretized beam section, material properties, and composite

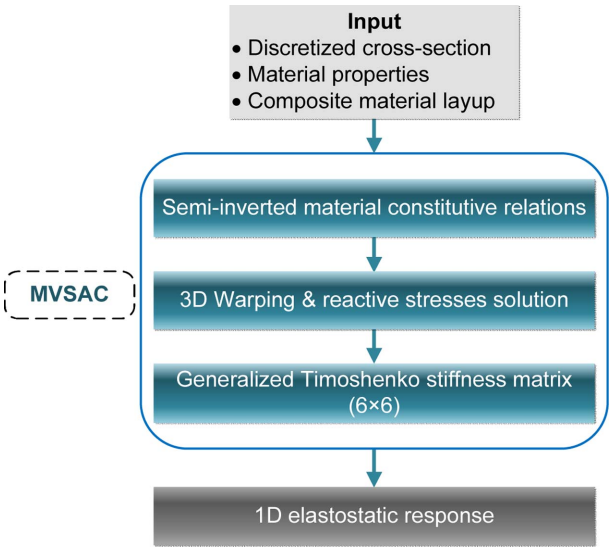

Fig. 2. Flowchart for the present cross-sectional analysis

layup are provided as input to the analysis. The semi-inverted material constitutive relations are first computed, as given in Eq. (10). The 3D warping deformation and reactive stress coefficients are then calculated using Eq. (27) which are used to compute the generalized 6×6 Timoshenko like stiffness matrix in Eq. (30).

3. RESULTS AND DISCUSSION

The present analysis MVSAC is validated for an elastically coupled composite box beam with a circumferentially anti-symmetric layup [6], as shown in Fig. 3. The material properties are given in Table 1 [6]. The section is discretized with 360 eight-node quadrilateral elements and 1,200 nodes giving a total of 7,200 degrees of freedom. The commercial software MSC Patran is used for the FE discretization. The section exhibits bending-torsion and extension-shear couplings.

3.1 Warping modes

The warping deformation modes computed by the present analysis are shown in Fig. 4. The extension-shear couplings results in an out-of-plane deformation in the extension (F_1) mode in addition to the in-plane component and leads to an in-plane deformation in the shear (F_2) mode. Because of the bending-torsion coupling, the bending (M_2) mode indicates additional out-of-plane deformation which is much dominant than the in-plane bending deformation. The shear (F_3) mode depicts only out-of-plane displacement and the bending (M_2) mode shows only in-plane displacement without any coupling contributions. These warping deformations are required for accurate computation of stiffness constants and the elastic couplings of the beam cross-section.

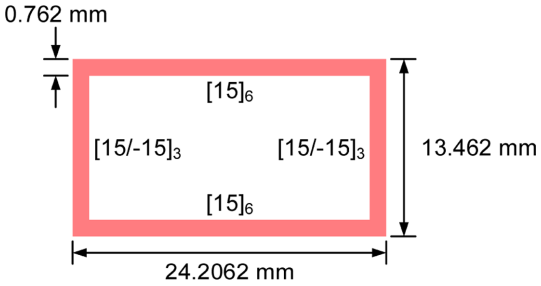

Fig. 3. Geometry and material layup of composite box beam

Table 1. Material properties for composite box beam

Property	Value
E_{11} (GPa)	141.9631
$E_{22} = E_{33}$ (GPa)	9.7906
$G_{12} = G_{13}$ (GPa)	6.1363
G_{23} (GPa)	4.7988
$\nu_{12} = \nu_{13} = \nu_{23}$	0.42

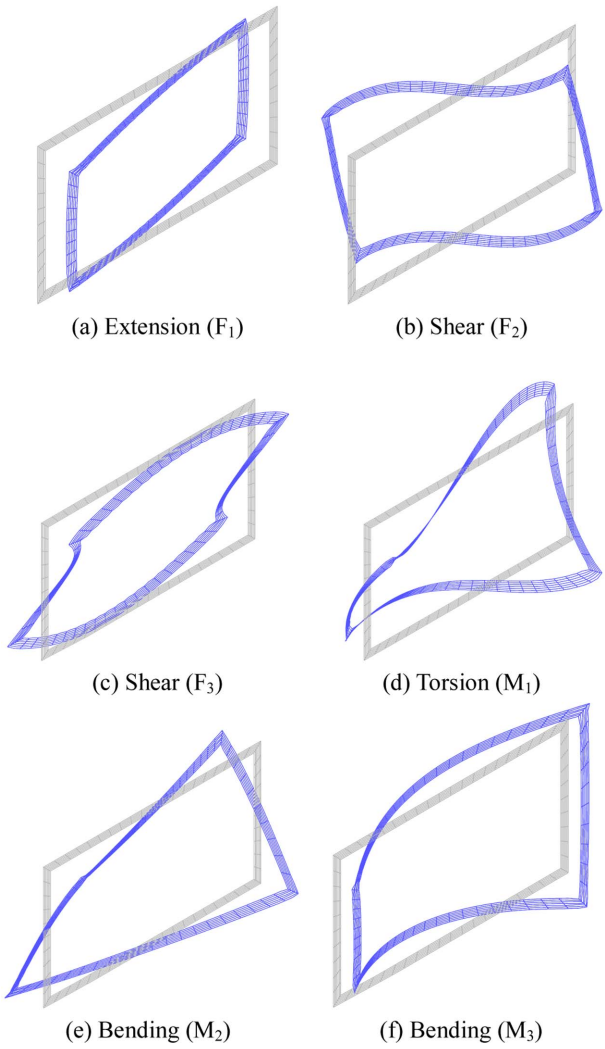

Fig. 4. Warping modes of composite box beam (exaggerated)

Table 2. Stiffness constants for composite box beam

Stiffness	Ref. [10]	Present	Difference (%)
$K_{11}\cdot10^6$ (N)	6.1270	5.9990	-2.09
$K_{12}\cdot10^5$ (N m)	8.1595	8.0840	-0.93
$K_{22}\cdot10^5$ (N)	3.9593	3.8939	-1.65
$K_{33}\cdot10^5$ (N)	1.7737	1.7191	-3.08
$K_{44}\cdot10^1$ (N m^2)	5.0099	4.9486	-1.22
$K_{45}\cdot10^1$ (N m^2)	-5.1554	-5.1015	-1.05
$K_{55}\cdot10^2$ (N m^2)	1.7524	1.7012	-2.92
$K_{66}\cdot10^2$ (N m^2)	4.1192	3.9649	-3.75

3.2 Stiffness constants

The sectional stiffness constants computed by the present multifield analysis are compared with those of displacement-based analysis [10] in Table 2. The present results match well with those of displacement-based analysis with maximum difference being 3.75% for the bending stiffness K_{66}. The exten-

Table 3. Response at mid-span under tip shear force

	Bending slope (rad)	Induced twist (rad)
Experiment [6]	8.155E-3	8.526E-3
MVSAC (present)	8.359E-3 (2.50)*	8.226E-3 (-3.52)
RDSAC [10]	8.025E-3 (-1.59)	7.913E-3 (-7.19)
Jung *et al.* [2]	8.054E-3 (-1.24)	8.384E-3 (-1.67)

*Percentage difference with respect to Experiment [6]

sion-shear K_{12} and bending-torsion K_{45} couplings show the differences of nearly 1%. Overall, a good correlation is achieved for all stiffness constants compared to the displacement-based approach [10]. The correct prediction of stiffness constants including any couplings is necessary for the computation of global 1D behavior of composite beams.

3.3 Elastostatic response

In order to investigate the accuracy of the present analysis, the 1D elastostatic response is computed for a cantilever beam of length L as 0.762 m. A vertical shear force F_3 of 4.448 N is applied at the tip end. The 1D elastostatic responses are computed through analytical expressions (see Ref. [10]).

Table 3 presents the comparison of bending slope and induced twist at the mid-span of the composite box beam. The present solution is compared with the experimental data [6], displacement-based analysis RDSAC [10], and Jung *et al.* [8]. The present value of the bending slope lies within 2.5% of that of the experimental value. The induced twist response obtained from RDSAC shows large difference whereas the present result is nearly 3.5% compared to the experimental data. Note that the experimental values (also shown in Fig. 5) indicate slight discrepancy which may be due to the measurement errors resulting from the imperfect boundary and loading fixtures. Fig. 5 shows the variation of the bending slope along the beam length. Overall, the present values are nearly identical to the experimental data [6] and indicate better correlation than those of RDSAC [10] and Jung *et al.* [8]. The comparison of induced twist along the beam length is presented in Fig. 6. The present multifield analysis matches well with the experimental data [6] except near the tip where the maximum deviation of 5.23% is noticed due to the nonuniform warping restraint effect which is neglected in the present approach. The induced twist computed by the present analysis performs better than the displacement-based RDSAC [10]. The elastostatic responses from the present multifield analysis show a good overall performance compared to other approaches because of soft response achieved through the multifield modeling of the sectional stresses and displacements.

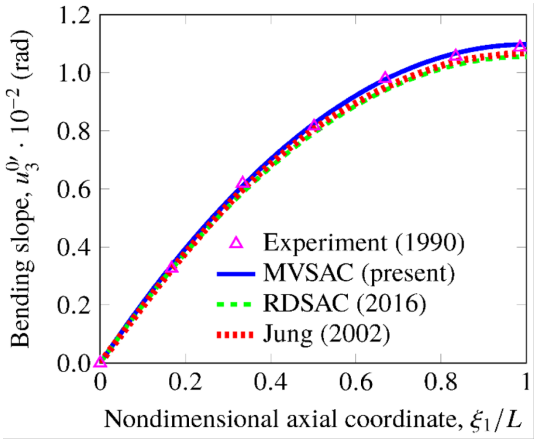

Fig. 5. Bending slope of composite box beam under tip shear force

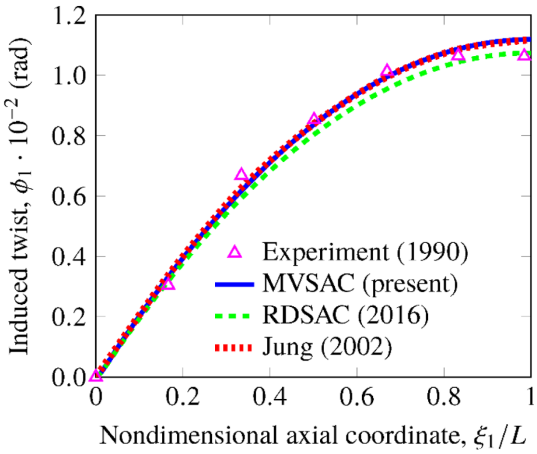

Fig. 6. Induced twist of composite box beam under tip shear force

4. CONCLUSIONS

A FE based multifield variational cross-sectional analysis is developed for nonhomogeneous composite beams considering reactive sectional stresses as unknowns. The analysis allows the modeling of beam cross-sections with arbitrary geometric layout and material distributions. The 3D warping deformations are illustrated for the successful prediction of elastic couplings for composite beams. The sectional stiffness constants obtained from the present multifield approach indicate deviations within 4% compared to the displacement-based approach. The elastostatic response computed using the present multifield analysis achieves an excellent correlation with the experimental data. The proposed cross-sectional analysis offers an alternative approach to model the composite beams such as rotor blades while considering the elastic coupling effects.

ACKNOWLEDGMENT

This research was supported by Basic Science Research Program through the National Research Foundation of Korea (NRF) funded by the Ministry of Education (2017R1D1A1A09000590). This work was conducted at High-Speed Compound Unmanned Rotorcraft (HCUR) research laboratory with the support of Agency for Defense Development (ADD).

REFERENCES

1. Hodges, D.H., "Unified Approach for Accurate and Efficient Modeling of Composite Rotor Blade Dynamics," *Journal of the American Helicopter Society*, Vol. 60, No. 1, 2015, pp. 1-28. doi: 10.4050/JAHS.60.011001
2. Jung, S.N., Nagaraj, V.T., and Chopra, I., "Assessment of Composite Rotor Blade Modeling Techniques," *Journal of the American Helicopter Society*, Vol. 44, No. 3, 1999, pp. 188-205. doi: 10.4050/JAHS.44.188
3. Giavotto, V., Borri, M., Mantegazza, P., Ghiringhelli, G., Carmaschi, V., Maffioli, G.C., and Mussi, F., "Anisotropic Beam Theory and Applications," *Computers and Structures*, Vol. 16, Nos. 1-4, 1983, pp. 403-413. doi: 10.1016/0045-7949(83)90179-7
4. Cesnik, C.E.S., and Hodges, D.H., "VABS: A New Cross-sectional Analysis," *Journal of the American Helicopter Society*, Vol. 42, No. 1, 1997, pp. 27-38. doi: 10.4050/JAHS.42.27
5. Berdichevsky, V.L., "Variational-asymptotic Method of Constructing a Theory of Shells," *Journal of Applied Mathematical Modelling*, Vol. 43, No. 4, 1979, pp. 711-736. doi: 10.1016/0021-8928(79)90157-6
6. Chandra, R., Stemple, A.D., and Chopra, I., "Thin-walled Composite Beams Under Bending, Torsional, and Extensional Loads," *Journal of Aircraft*, Vol. 27, No. 7, 1990, pp. 619-626. doi: 10.2514/3.25331
7. Chandra, R., and Chopra, I., "Structural Response of Composite Beams and Blades with Elastic Couplings," *Composites Engineering*, Vol. 2, Nos. 5-7, 1992, pp. 347-374. doi: 10.1016/0961-9526(92)90032-2
8. Jung, S.N., Nagaraj, V.T., and Chopra, I., "Refined Structural Model for Thin- and Thick-walled Composite Rotor Blades," *AIAA Journal*, Vol. 40, No. 1, 2002, pp. 105-116. doi: 10.2514/2.1619
9. Reissner, E., "On Mixed Variational Formulations in Finite Elasticity," *Acta Mechanica*, Vol. 56, Nos. 3-4, 1985, pp. 117-125. doi: 10.1007/BF01177113
10. Dhadwal, M.K., and Jung, S.N., "Refined Sectional Analysis with Shear Center Prediction for Nonhomogeneous Anisotropic Beams with Nonuniform Warping," *Meccanica*, Vol. 51, No. 8, 2016, pp. 1839-1867. doi: 10.1007/s11012-015-0338-2.